



Critical role of Erythrocyte Binding-Like protein of the rodent malaria parasite *Plasmodium yoelii* to establish an irreversible connection with the erythrocyte during invasion



Yuto Kegawa^{a,b}, Masahito Asada^{a,b}, Takahiro Ishizaki^{a,b}, Kazuhide Yahata^b, Osamu Kaneko^{a,b,*}

^a Program for Nurturing Global Leaders in Tropical and Emerging Communicable Diseases, Graduate School of Biomedical Sciences, Nagasaki University, 1-12-4 Sakamoto, Nagasaki 852-8523, Japan

^b Department of Protozoology, Institute of Tropical Medicine (NEKKEN), Nagasaki University, 1-12-4 Sakamoto, Nagasaki 852-8523, Japan

ARTICLE INFO

Keywords:

EBL
Erythrocyte
Invasion
Malaria
Plasmodium yoelii
Time-lapse imaging

ABSTRACT

Plasmodium malaria parasites multiply within erythrocytes and possess a repertoire of proteins whose function is to recognize and invade these vertebrate host cells. One such protein involved in erythrocyte invasion is the micronemal protein, Erythrocyte Binding-Like (EBL), which has been studied as a potential target of vaccine development in *Plasmodium vivax* (PvDBP) and *Plasmodium falciparum* (EBA-175). In the rodent malaria parasite model *Plasmodium yoelii*, specific substitutions in the EBL regions responsible for intracellular trafficking (17XL parasite line) or receptor recognition (17X1.1pp. parasite line), paradoxically increase invasion ability and virulence rather than abolish EBL function. Attempts to disrupt the *eb1* gene locus in the 17XL and 17XNL lines were unsuccessful, suggesting EBL essentiality. To understand the mechanisms behind these potentially conflicting outcomes, we generated 17XL-based transfectants in which *eb1* expression is suppressed with anhydrotetracycline (ATc) and investigated merozoite behavior during erythrocyte invasion. In the absence of ATc, EBL was secreted to the merozoite surface, whereas following ATc administration parasitemia was negligible *in vivo*. Merozoites lacking EBL were unable to invade erythrocytes *in vitro*, indicating that EBL has a critical role for erythrocyte invasion. Quantitative time-lapse imaging revealed that with ATc administration a significant number of merozoites were detached from the erythrocyte after the erythrocyte deformation event and no echinocytosis was observed, indicating that EBL is required for merozoites to establish an irreversible connection with erythrocytes during invasion.

1. Introduction

Human malaria is a life-threatening disease with > 200 million new cases and > 400,000 deaths annually [1]. Malaria symptoms and pathogenesis are caused by blood stage *Plasmodium* parasites, for which invasion into and schizogony within the erythrocyte is essential for their proliferation in the host. Erythrocyte invasion is a rapid and complex process consisting of sequential and specific molecular interactions between the parasite and erythrocyte molecules [2–4]. During invasion initiation the merozoite reversibly binds to the erythrocyte and reorients its anterior end in contact with the erythrocyte membrane. This step is called the pre-invasion phase and is characterized by dramatic erythrocyte deformation. After reorientation, the merozoite establishes an irreversible connection, *via* a tight junction structure,

between the parasite anterior end and the erythrocyte membrane. During invasion the merozoite moves into a nascent membranous structure termed a parasitophorous vacuole formed in the erythrocyte. Finally, the erythrocyte aggressively deforms and spike-like structures transiently appear on its surface, before returning to a normal shape within 10 min [5, 6]. This step is called echinocytosis and is proposed to be stimulated by an efflux of erythrocyte potassium and chloride ions [6].

Many parasite molecules involved in the erythrocyte invasion process have been identified; however, the precise function of most parasite molecules and relationships between erythrocyte molecules during invasion are not fully understood. One of the best-characterized merozoite ligands is the Erythrocyte Binding-Like (EBL) family protein, which is secreted from micronemes following calcium signaling

* Corresponding author at: Department of Protozoology, Institute of Tropical Medicine (NEKKEN), Nagasaki University, 1-12-4 Sakamoto, Nagasaki 852-8523, Japan.

E-mail addresses: yuto.kegawa@yahoo.co.jp (Y. Kegawa), masahitoasada@nagasaki-u.ac.jp (M. Asada), takahiro.ishizaki.0616@gmail.com (T. Ishizaki), kyahata@nagasaki-u.ac.jp (K. Yahata), okaneko@nagasaki-u.ac.jp (O. Kaneko).

<https://doi.org/10.1016/j.parint.2018.07.006>

Received 4 June 2018; Received in revised form 13 July 2018; Accepted 14 July 2018

Available online 17 July 2018

1383-5769/ © 2018 The Authors. Published by Elsevier B.V. This is an open access article under the CC BY-NC-ND license (<http://creativecommons.org/licenses/by-nc-nd/4.0/>).

induction upon merozoite egress from the infected erythrocyte [7]. A primate and zoonotic malaria parasite *Plasmodium knowlesi* uses one EBL family member to recognize Duffy Antigen Receptor for Chemokines (DARC) on human erythrocyte and electron microscopic images suggested a lack of DARC in variant erythrocytes affected the tight junction formation between the parasite and the erythrocyte membrane [8, 9]. *Plasmodium falciparum*, the causative agent of malignant human malaria, expresses multiple EBL family proteins (namely, EBA-175, EBA-181, EBA-140, and EBL1) with different receptor specificities. This diversity of receptors allows recognition of variant human erythrocytes lacking specific surface ligands, and thus disruption of one EBL member in *P. falciparum* usually does not show a lasting invasion phenotype for invasion of normal erythrocytes [10–14].

Plasmodium yoelii, a rodent malaria parasite, has been widely used to study many aspects of host-parasite interactions and possesses only one EBL [15]. In this *Plasmodium* species, specific single amino acid substitutions of EBL result in a switch in erythrocyte preference from reticulocyte to normocyte, and thereby great differences in virulence between 17XL and 17XNL, or 17X1.1pp. and CU lines [16–18]. EBL in the 17XL line *P. yoelii* traffics to dense granules, due to a mutation of one out of 8 conserved Cys residues within an EBL domain (region 6) responsible for wild type intracellular microneme targeting of EBL family members. In the 17XL line it has not been determined if dense granule localization results in EBL secretion to the merozoite surface and functional recognition of the host erythrocyte receptor [16]. In a second study, a genetic cross between 17 × 1.1 pp. and CU line parasites showed that one out of 12 Cys residues, conserved among EBL family members in the domain (region 2) responsible for receptor recognition, also altered parasite virulence. In contrast to the above 17XL mutation, a disruption or alteration of the EBL receptor interaction with the erythrocyte surface was the apparent determinant of this phenotypic change of the 17 × 1.1 pp. parasite line. Taken together, the fact that mutations which appear to disrupt normal EBL function are not lethal, and indeed increase virulence, suggest that EBL is not essential for *P. yoelii*. However, efforts to disrupt the *eb1* gene locus in the 17XL and 17XNL lines by homologous recombination have been unsuccessful, suggesting an essentiality of *eb1* in both parasite lines [16].

Recently, a tetracycline-repressive transactivator (Tet-Off) system was reported in *P. falciparum* and the rodent malaria parasite *Plasmodium berghei*, which was able to reduce the expression of target genes by up to 95% [19]. In this strategy, a fusion protein composed of the Tet repressor (TetR) and a modified *Plasmodium* ApiAP2 transactivation domain (ranTRAD4 in this manuscript) is introduced immediately upstream of the gene of interest. The promoter of the target gene is thus replaced by a minimal promoter containing a repeated Tet operator (TetO) sequence, which serves as a binding site for the TetR/ranTRAD4 fusion protein. This fusion protein binds anhydrotetracycline (ATc) and transcription of the targeted gene is down-regulated under the presence of ATc. In this study we used the Tet-Off system to study EBL function via regulation of *eb1* expression in the *P. yoelii* 17XL line. In the absence of ATc, EBL is secreted onto the surface of merozoites in both 17XL and 17XNL parasite lines. Conditional knockdown of EBL in the presence of ATc severely reduces parasite growth and erythrocyte invasion, and thus EBL appears to be essential within the experimental timeframe of an ATc knockdown experiment. Using time-lapse imaging we quantitatively demonstrate that merozoites are not able to establish an irreversible connection with erythrocytes and detach after the deformation of erythrocytes.

2. Material and methods

2.1. Parasites and experimental animals

The *P. yoelii* 17XL parasite line was maintained in the Institute of Tropical Medicine, Nagasaki University, participating in the National Bio-Resource Project of the MEXT, Japan. Female 6–8 weeks old ICR

mice (Japan SLC) were used for parasite propagation. Animal experiments were approved by the Animal Care and Use Committee of Nagasaki University (Permit number 1403031120-9).

2.2. Plasmid construction

A plasmid containing the Tet-Off-based inducible mCherry expression cassette (PyTet-Off-mCherry-plasmid) was constructed using the Multisite Gateway® system (Invitrogen, Carlsbad, CA, USA). Components for Tet-Off were PCR-amplified from genomic DNA (gDNA) of a *P. berghei* line whose mCherry signal is controlled under ranTRAD4 (a kind gift from Dr. Soldati-Favre) [19]. Firstly, we constructed three entry plasmids: pENT41-ef1 α containing *P. berghei* elongation factor 1 α promoter sequence (amplified from pHDEF-*luc* [20]); pENT12-TetR/HSP86-3 U containing TetR/ranTRAD4 and *P. falciparum* heat shock protein 86 terminator sequence (amplified from pDST43-HDEF-F3 [17]); and pENT23-TetO/mCherry containing TetO4, *P. falciparum* calmodulin minimal promoter, and mCherry sequences. pCHD43(II) was used as a destination plasmid [21, 22]. The sequences for 5'- and 3'-homologous recombination to integrate into the *p230* locus were amplified from *P. yoelii* 17XL gDNA and inserted into the *KpnI* and *AatII* sites, respectively, of pCHD43(II) plasmid using an In-Fusion HD Cloning Kit (Takara Bio Inc., Japan). Entry and destination plasmids were recombined by the Gateway LR reaction, linearized with *SacI* and *NaeI*, and used for transfections.

To generate plasmids designed to be integrated into the *eb1* gene locus, in which TetR/ranTRAD4 transcription is regulated by the *P. yoelii* *eb1*, *ron2*, or *rhoph2* promoters, the respective promoter sequences were PCR-amplified from *P. yoelii* gDNA for insertion into pENT41-based entry plasmids. Tet-Off components were amplified from gDNA of *mCherry-KD* parasites to generate pENT13-TetR/CAM containing TetR/ranTRAD4, *hsp86* terminator, TetO4, and CAM minimal promoter sequences. The sequences for 5'- and 3'- homologous recombination to integrate into the *eb1* locus were amplified from *P. yoelii* 17XL gDNA and inserted into the *XhoI* and *HpaI* sites, respectively, of pCHD43(II). These plasmids were then recombined by the Gateway LR reaction and linear DNA fragments were prepared by PCR-amplification for transfection. All primers used for plasmid construction are shown in Table S1.

2.3. Parasite transfection

Schizonts were enriched by centrifugation over a Histodenz density cushion. Histodenz™ (Sigma-Aldrich, St. Louis, MO) solution was prepared as 27.6 g/100 mL in Tris-buffered solution (5 mM Tris-HCl, 3 mM KCl, and 0.3 mM CaNa₂-EDTA, pH 7.5) then diluted with equal volume of RPMI1640-based incomplete medium containing 25 mM HEPES and 100 mg/L of hypoxanthine [23]. The schizont-enriched parasites were transfected using a Nucleofector™ 2b device (Lonza Japan) as described [24]. For each transfection we used 20 μ g of linearized plasmids or PCR-amplified linear DNA fragments. Stable transfectants were selected by oral administration of pyrimethamine and cloned by limiting dilution in mice.

2.4. Southern Blotting

For Southern blotting, gDNA was digested with *AatII* and *NheI* and separated by 1% agarose gel electrophoresis. Gels were treated with denaturing solution (1.5 M NaCl and 0.5 M NaOH) for 35 min and neutralization solution (1.5 M NaCl and 0.5 M Tris-HCl, pH 7.5) for 30 min, then the DNA fragments were transferred onto nylon membrane (Amersham Hybond-N⁺; GE Healthcare, Buckinghamshire, UK) and hybridized with specific DNA probes. DNA probes were PCR-amplified from *P. yoelii* 17XL gDNA with specific primers (listed in Table S1) and treated with AlkPhos Direct Labelling and Detection System (GE Healthcare) according to the manufacturer's instructions. Probes were hybridized to membranes in pre-warmed hybridization buffer

(0.5 M NaCl, 4% w/v blocking reagent). Hybridized probes were detected with CDP-Star® Detection Reagent (GE Healthcare) and luminescence was detected by a biomolecular imager (ImageQuant LAS 4000 mini, Fujifilm, Japan).

2.5. Anhydrotetracycline (ATc) treatment

ATc (Sigma-Aldrich) was dissolved in 5% sucrose water at a concentration of 0.2 mg/mL and orally administered to mice infected with *mCherry-KD* transgenic parasites. New solutions of ATc were supplied every 48 h [19]. For mice infected with *eb1-KD* transgenic lines, 500 µL of PBS containing 2 mg of ATc was subcutaneously injected every 24 h after the parasitemia reached 1%, and the same volume of PBS was injected into the negative control group.

2.6. Monitoring of parasitemia and stage transition

Parasitemia was calculated by examining at least 10,000 erythrocytes or 100 parasite-infected erythrocytes for each Giemsa-stained blood smear. Statistical analysis of parasitemias during the parasite growth *in vivo* was conducted using the two-way repeated measures ANOVA and Tukey's test. Parasite stages were classified into ring, small late trophozoite, large late trophozoite, and schizont stages. Small versus large late trophozoites were distinguished based upon diameter; specifically, < 50% of erythrocyte diameter versus ≥ 50%, respectively. Schizonts were defined as parasites with more than one nucleus. We examined 200 infected erythrocytes to determine the ratio of the different stages 0, 12, and 18 h after ATc treatment.

2.7. RNA extraction, cDNA synthesis, and quantitative reverse-transcription polymerase chain reaction (qRT-PCR)

To evaluate *eb1* transcription levels after ATc administration, *eb1-KD* parasites were collected from mice 12 h after ATc administration and treated with 0.15% saponin (Sigma-Aldrich) in PBS. Parasite pellets were suspended in TRIzol reagent (Thermo Fisher Scientific, Waltham, MA) and total RNA was extracted according to the manufacturer's instructions. Total RNA was treated with DNase I (Invitrogen) and further purified using SV Total RNA Isolation System (Promega, Madison, WI), then again treated with DNase I. Complementary DNA (cDNA) synthesis was performed using SuperScript III (Invitrogen) according to the manufacturer's instructions. qRT-PCR was performed to quantitate transcripts of *eb1* and *ama1* with Power SYBR™ Green PCR Master Mix (Thermo Fisher Scientific) and specific primer sets (listed in Table S1) using the 7500 Real-Time PCR system (Applied Biosystems, Foster City, CA). Values for *eb1* transcripts were normalized to those for *ama1* transcripts and values from three independent experiments were compared by the one-tailed Student's *t*-test.

2.8. SDS-PAGE, Western blotting and quantification of EBL protein

Schizonts were enriched by Histodenz density cushions as above, then the number of schizonts were adjusted to 1.0×10^8 per sample. Proteins were first extracted by repeated freeze-thaw cycles in PBS containing protease inhibitors (PBS-PI; cOmplete™ EDTA-free, Sigma-Aldrich). After centrifugation, supernatants were removed and pellets were dissolved in 50 µL of PBS-PI with 1% Triton X-100. Five microliters of Triton X-100-soluble fractions, containing EBL and AMA1, were separated by polyacrylamide gel electrophoresis (5–20%; ATTO, Japan) under reducing conditions, then transferred onto polyvinylidene fluoride membranes (Clear Blot membrane-P; ATTO). Membranes were immunostained with rabbit anti-PyEBL antiserum (1:4000 dilution) [16] or mouse anti-PyAMA1 antiserum (1:300 dilution) [25], followed by HRP-conjugated anti-rabbit IgG or anti-mouse IgG (1:25000 dilution; Promega), respectively. The signals were developed with Immobilon Western Chemiluminescent HRP Substrate (Millipore) and

detected by a biomolecular imager. The obtained protein band signals were quantified by Multi Gauge software (Fujifilm) and evaluated by the Chi-square test.

2.9. Indirect immunofluorescent assay (IFA)

Mature enriched schizonts were suspended in 1 mL of RPMI1640-based complete media (supplemented with 25 mM HEPES, 0.225% sodium bicarbonate, 0.1 mM hypoxanthine, 10 mg/mL gentamicin, and 1% AlbuMax I, pH 7.4) at 15 °C, and filtered through a filter unit with a 1.2 µm pore size (Sartorius Stedim Biotech, Göttingen, Germany). Purified merozoites were used for IFA analysis immediately, or following incubation at 37 °C for 10 min using a shaking incubator (Thermomixer® comfort; Eppendorf, Hamburg, Germany) [23]. Merozoites were fixed with 4% paraformaldehyde and 0.0075% glutaraldehyde for 10 min, placed on a poly-L-lysine-coated cover glass and kept for 30 min, then incubated in PBS with 3% BSA for 1 h. Anti-PyMSP1 chicken serum (1:500 dilution) [23] and anti-PyEBL rabbit serum (1:250 dilution) [16] were reacted at room temperature for 1 h and Alexa fluor 488-conjugated goat anti-chicken IgY antibody (1:1000 dilution) and Alexa fluor 647-conjugated goat anti-rabbit IgG antibody (1:1000 dilution) were reacted at room temperature for 30 min. Parasite nuclei were stained with 4', 6-diamidino-2-phenylindole (DAPI; Invitrogen). Cover slips were mounted with ProLong® Gold antifade reagent (Invitrogen) and placed on microscope glass slides. All IFA images were obtained with a confocal microscope (Nikon A1; Nikon, Japan) and processed using Adobe Photoshop CS (Adobe systems Inc., San Jose, CA).

2.10. Erythrocyte invasion assay

Merozoites were isolated and invasion assays were performed as described [23]. In brief, mature enriched schizonts were suspended in 1 mL of RPMI1640-based complete media at 15 °C, and filtered through a filter unit with a 1.2 µm pore size. The yielded filtrate containing approximately 1.0×10^6 or more free merozoites was mixed with 5.0×10^7 uninfected erythrocytes pre-warmed to 37 °C. Mixtures were incubated at 37 °C for 1 h with shaking at 1000 rpm using a shaking incubator (Thermomixer® comfort), then further incubated at 37 °C in the 96 well plate with 5% O₂, 5% CO₂, and 90% N₂ gas mixture for 18 h. Parasitemia was calculated by examining at least 10,000 erythrocytes or 100 parasite-infected erythrocytes for each Giemsa-stained blood smear.

2.11. Time-lapse imaging

ATc or PBS was subcutaneously administered to mice infected with *eb1-KD* transgenic parasite lines at 4 to 6 days post-inoculation when parasitemias reached > 30%. Whole blood was collected 12 h after ATc or PBS administration. Schizonts were enriched on Histodenz density cushions, suspended in 1 mL of complete medium, and incubated at 15 °C with 5% O₂, 5% CO₂, and 90% N₂ gas mixture for 3 h. Merozoites were isolated as described [23] and kept at 15 °C. Mouse fresh erythrocytes were adjusted to 25,000 erythrocytes/µL with RPMI1640-based complete media pre-warmed to 37 °C. Erythrocyte solutions were transferred to µ-Slide VI 0.4 (ibidi, Germany) chambers, and purified merozoites were then added and kept at room temperature for 10 min to allow the merozoites to settle to the bottom of the chamber. Slides were placed on the stage of an inverted microscope (Ti-E; Nikon, Japan) and video images were captured using a 60× oil objective lens (N.A. 1.4). The microscope was configured for stable time-lapse imaging with a perfect focus system (Nikon). The water chamber stage (Tokai Hit, Japan) and the objective lens were kept at 37 °C with a temperature controller (Tokai Hit). Time-lapse images were captured every 0.1 s up to 40 min using a CCD camera (ORCA-R2; Hamamatsu Photonics, Japan) and imaged using NIS-Element Advanced Research imaging

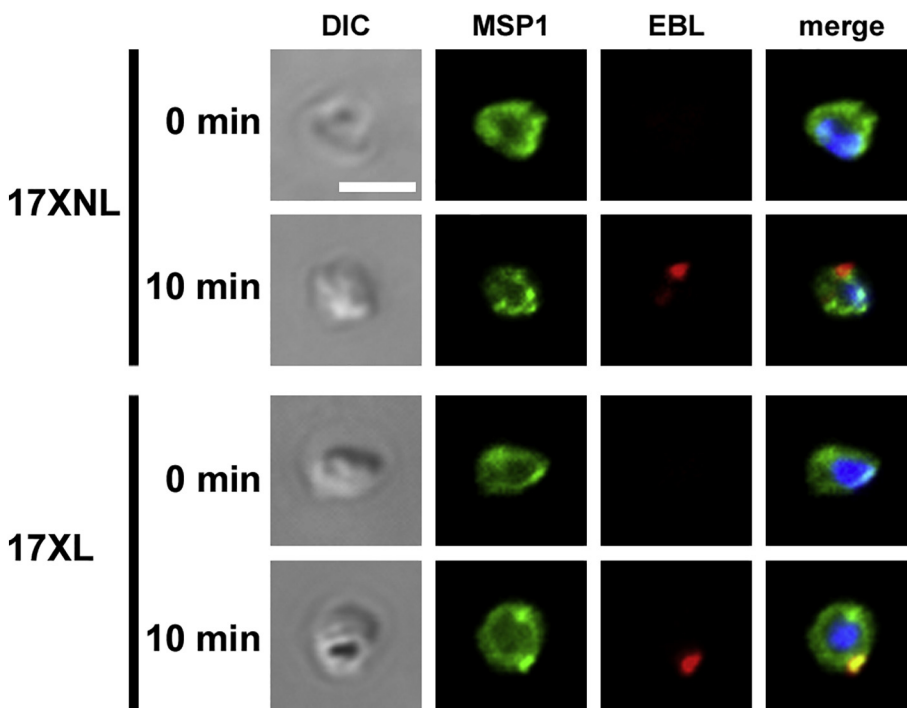


Fig. 1. EBL translocates to the merozoite surface in *P. yoelii* 17XL and 17XNL lines. Merozoites were immunostained immediately after purification (0 min) or after incubating at 37 °C for 10 min. DIC, Differential Interference Contrast image; EBL (red), Erythrocyte-Binding-Like protein; MSP1 (green), a merozoite surface marker Merozoite Surface Protein 1. Merged images of MSP1, EBL, and DAPI (nucleus staining) are shown (merge). Bar = 2 μm. (For interpretation of the references to colour in this figure legend, the reader is referred to the web version of this article.)

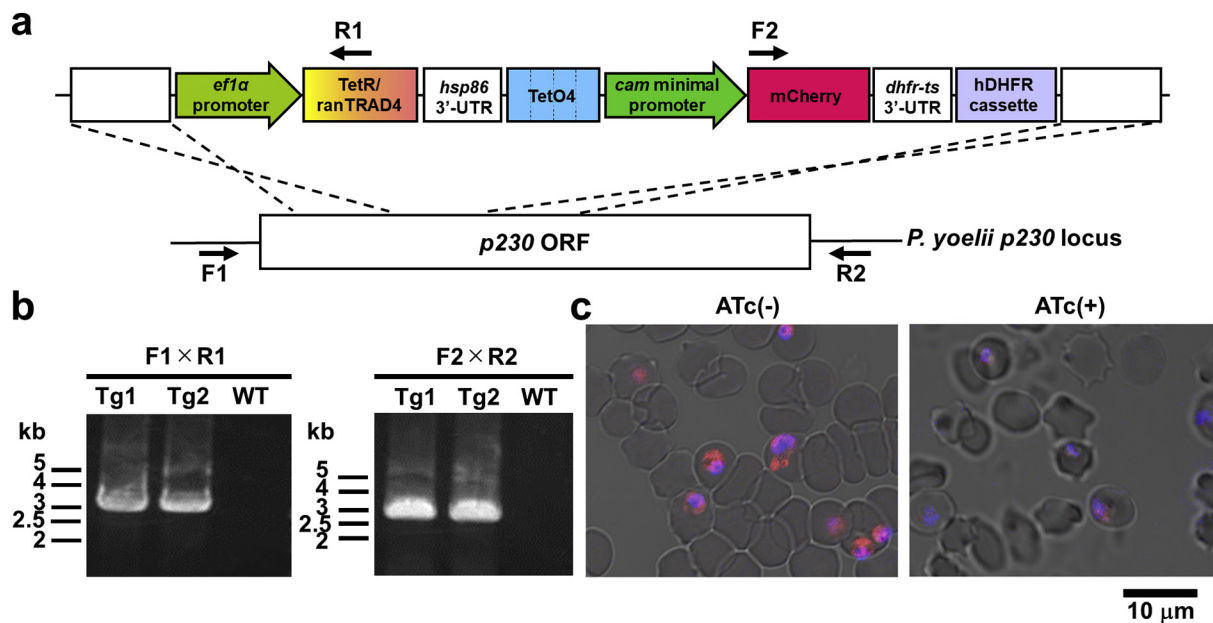


Fig. 2. Evaluation of Tet-Off system in *P. yoelii*. (a) Schematic of the plasmid to generate a *mCherry*-KD parasite line (not drawn to scale). The Tet-Off cassette was designed to be integrated into the *P. yoelii* *p230* gene locus. *Cam*, *P. falciparum* calmodulin; *dhfr-ts*, *P. berghei* dihydrofolate reductase-thymidylate synthase; *ef1a*, *P. berghei* elongation factor 1 α ; hDHFR cassette, human DHFR controlled by *P. falciparum* calmodulin promoter and histidine-rich protein 2 terminator; *hsp86*, *P. falciparum* heat shock protein 86; TetO4, 4 repeats of the Tetracycline Operator sequence; TetR/ranTRAD4, Tetracycline Repressor fused with randomized TransActivating Domain. Target location of the diagnostic PCR primers are shown (F1, R1, F2, and R2) (b) Diagnostic PCR. Bands with expected sizes at 3.1 kb (F1 and R1) or 2.8 kb (F2 and R2) were obtained for two independently generated *mCherry*-KD transgenic lines (Tg1 and Tg2). No band was detected from wild type parasites (WT). (c) *mCherry* signals were weak in the *mCherry*-KD Tg1 line 4 days after continuous oral ATc administration (ATc(+)), whereas clear signals were observed in a group without ATc administration (ATc(-)). Images were captured under the same condition. Bar = 10 μm.

software (Nikon) [4]. The videos were converted to 2 fps with AviUtil software (<http://spring-fragrance.mints.ne.jp/aviutil/>) and analyzed. Fisher's exact test was used to compare the frequency of each invasion event. Mann-Whitney *U* test was used to compare the duration of each invasion event.

3. Results

3.1. EBL is translocated to the merozoite surface in *P. yoelii* 17XL and 17XNL lines

To determine if EBL is translocated to the merozoite surface of the 17XL parasite line, we performed IFA with anti-EBL antibody using

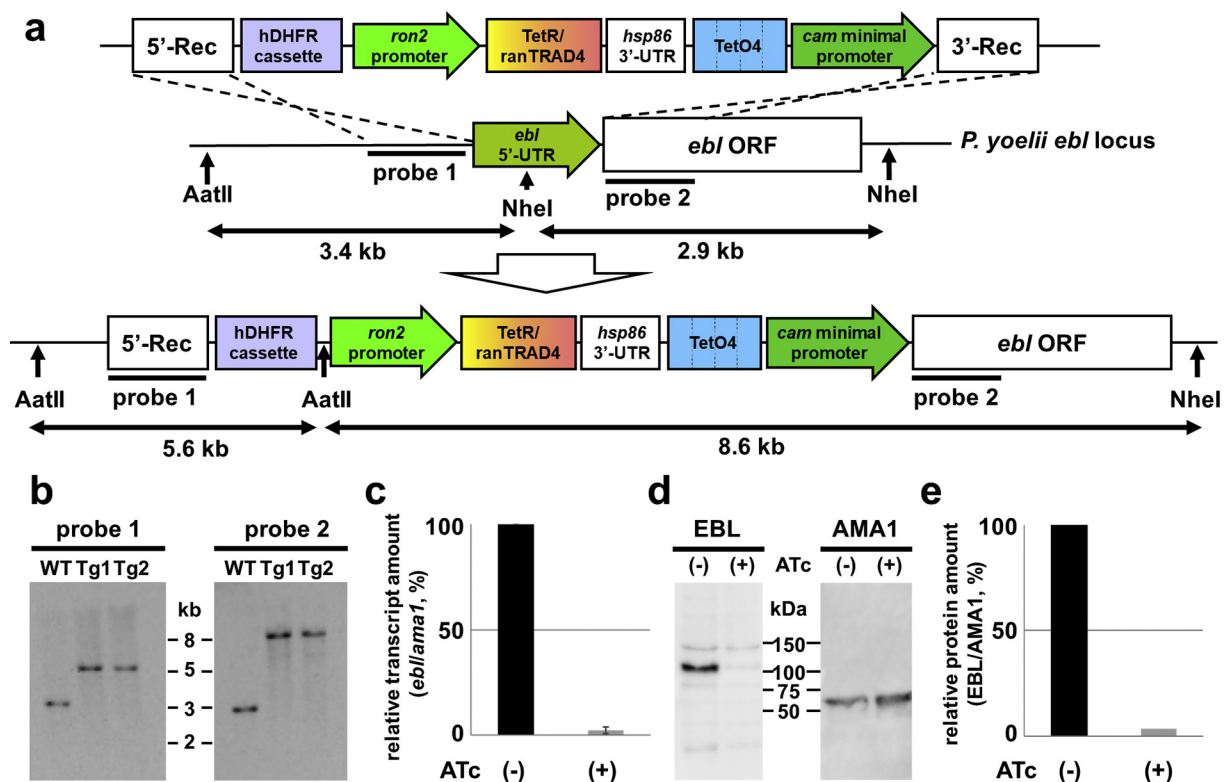


Fig. 3. Generation of *P. yoelii* transgenic lines for which *ebl* can be knocked down. (a) Schematic of the plasmid to generate *ebl*-KD parasite lines (not to scale). The gene encoding TetR/ranTRAD4 fusion protein is transcribed under *P. yoelii* *rhoph2*, *ron2*, or *ebl* promoter (only *ron2* is shown). *ebl* 5'-UTR, *ebl* ORF, 5'-Rec, and 3'-Rec are 5' untranslated region and open reading frame of *ebl* gene, and the regions used for the homologous recombination. *AatII* and *NheI* restriction sites with the expected distance between sites are shown. Target location of the Southern blot probes (probe 1 and 2) are shown. See Fig. 2 legend for abbreviations of the plasmid components. (b) Southern blot analysis. Both probes detected single bands in a parental parasite line (WT) at 3.4 kb with the probe 1 and at 2.9 kb with the probe 2, whereas *ebl*-KD Tg1 and Tg2 lines showed bands at 5.6 kb with the probe 1 and at 8.6 kb with the probe 2. (c) Quantitative Reverse Transcription-PCR. The value of *ebl* transcripts were normalized by that of *ama1* transcripts. *Ebl* transcripts were significantly lower in the ATc(+) group than the ATc(-) group 12 h after ATc administration ($p < .05$, one-tailed Student's *t*-test). Bars indicate standard deviation from triplicates. (d) Western blot analysis. Parasite proteins were extracted with Triton X-100 from schizonts and reacted with anti-PyEBL or anti-PyAMA1 antibodies. A clear band was detected around 100 kDa corresponding to EBL in the ATc(-) group, whereas only a faint band was observed in the ATc(+) group. AMA1 was used as a loading control. (e) The amount of EBL was < 5% in the ATc(+) group, dramatically lower than the ATc(-) group. Intensity of the EBL bands in the panel (d) was normalized by that of AMA1 bands.

non-permeabilized merozoites purified by our recently established method to isolate invasive merozoites [23]. We found that EBL surface signal was not detectable on merozoites immediately after purification, whereas they became positive as a confined dot at one area on merozoites after incubating at 37 °C for 10 min for both 17XL and 17XNL lines (Fig. 1). This result indicates that EBL is translocated to the merozoite surface after egress from the infected erythrocyte in the *P. yoelii* 17XL line despite its intracellular localization to dense granules, suggesting that EBL might have the opportunity to encounter its cognate erythrocyte receptor in this parasite line in the absence of regulated release from micronemes.

3.2. Establishment of Tet-Off system in *P. yoelii*

To adapt the ATc inducible Tet-Off system to the *P. yoelii* 17XL line, we introduced a Tet-Off-based inducible mCherry expression cassette into the *p230* gene locus (Fig. 2a). The genome integration of the construct in the resulting transfectant, termed *mCherry*-KD, was confirmed by diagnostic PCR (Fig. 2b). To determine the effect of ATc on mCherry expression, *mCherry*-KD parasites were inoculated into mice with or without ATc treatment. Fluorescence microscopy of the parasite at day 4 after inoculation revealed that the mCherry signal in the ATc(+) group (collected from mice treated with ATc every day from 2 days before parasite inoculation) was much weaker than that in the control ATc(-) group, indicating functional integration of the Tet-Off cassette in the *P. yoelii* line and appropriate suppression of mCherry expression

by ATc administration (Fig. 2c).

3.3. Successful knockdown of EBL in the *P. yoelii* 17XL line

Next, we generated a construct that would express TetR/ranTRAD4 fusion protein under the endogenous *ebl* promoter; however, we failed to obtain integrant parasites. We hypothesized that this could be due to an imbalance of the expression level between TetR/ranTRAD4 protein and the target protein driven by *tet operator* (*TetO*) within a calmodulin minimal promoter. To this end, we examined the expression level of TetR/ranTRAD4 and mCherry in *mCherry*-KD parasites and found that the amount of *mCherry* transcripts was much lower than that of TetR/ranTRAD4 transcripts in this parasite (Supplement 1), suggesting that the transcription level of the target gene by our initial design is likely reduced, which in turn affects parasite survival. To overcome this potential problem, we made 3 plasmids designed to be integrated into the *ebl* gene locus, for which TetR/ranTRAD4 transcription is regulated under the *P. yoelii* *ebl*, *ron2*, or *rhoph2* promoters - all of which are transcribed at the schizont stage. We selected promoters for these genes because the transcription level of the *ron2* and *rhoph2* were 1.3- and 3-fold higher than that of *ebl* in *P. yoelii*, respectively (unpublished data). As a result, we reproducibly obtained transgenic parasite lines with the *ron2* promoter-based plasmid, but not with *ebl* and *rhoph2* promoter-based plasmids. Two independently generated transfectant lines were termed *ebl*-KD Tg1 and Tg2 (Fig. 3a). Integration of the Tet-Off cassette into the *ebl* gene locus was confirmed by Southern blot analysis

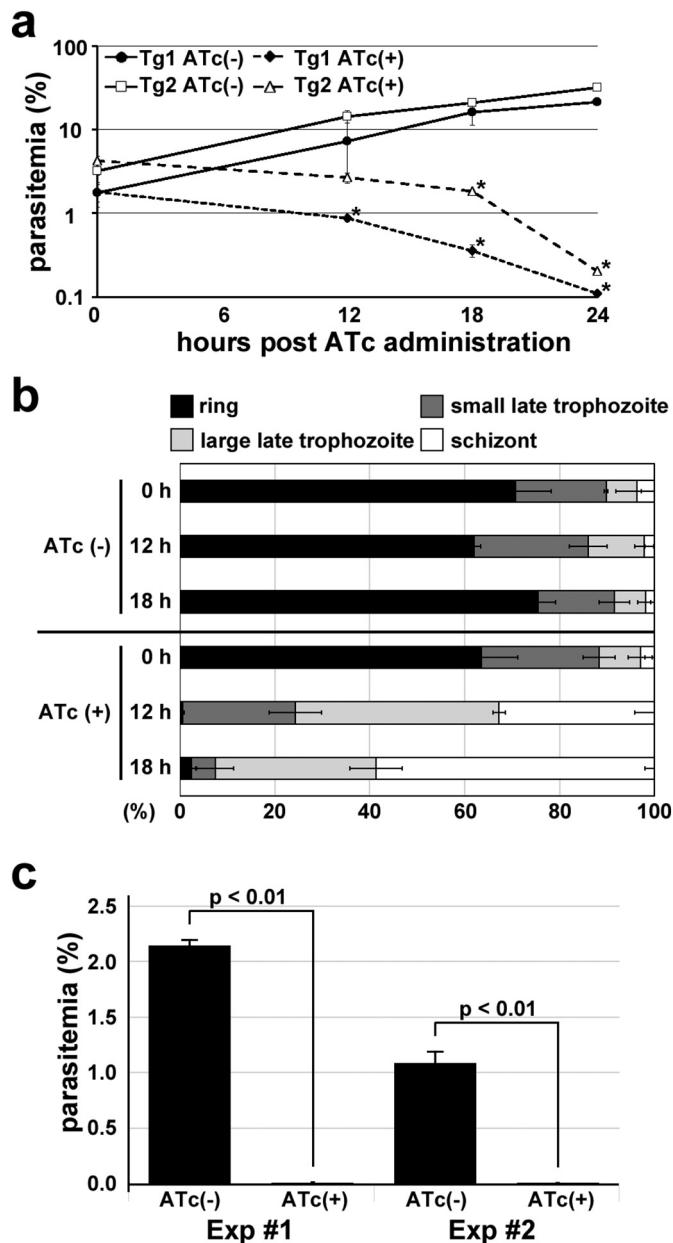


Fig. 4. Effect of the knockdown of *ebl* on parasite growth and erythrocyte invasion. (a) Parasitemia were monitored 0, 12, 18, and 24 h after ATc (or control PBS) administration for Tg1 and Tg2 lines with (ATc(+)) or without (ATc(-)) ATc administration. Asterisk indicates the parasitemia of the ATc(+) group significantly lower than that of the ATc(-) group ($p < .01$, Tukey's test). (b) Proportion of ring, small late trophozoites, large late trophozoites, and schizont stages obtained 0, 12, and 18 h after ATc (or control PBS) administration. (c) Invasion ability of *ebl*-KD Tg1 merozoites. The ATc(+) group repeatedly showed significantly lower values than the ATc(-) group ($p < .01$, one-tailed Student's t-test). Bars indicate standard deviation from triplicates.

(Fig. 3b). The amount of *ebl* transcripts in the ATc(+) group was $< 5\%$ of that in the ATc(-) control group 12 h after ATc administration (Fig. 3c). By Western blot analysis, control AMA1 protein was clearly seen in both ATc(-) and ATc(+) groups, whereas a 110-kDa band corresponding to EBL was detected in the ATc(-) group but barely visible in the ATc(+) group (Fig. 3d). The amount of EBL protein in the ATc(+) group was $< 5\%$ of that in the ATc(-) group 12 h after ATc administration (Fig. 3e). These results indicate that *ebl* transcription and EBL protein expression in *P. yoelii* were efficiently reduced by ATc administration.

3.4. Loss of *ebl* in the *P. yoelii* 17XL line resulted in unsuccessful erythrocyte invasion

Next, we examined the effect of *ebl* knockdown on parasite growth. *Ebl*-KD parasites grow as efficiently as the parental 17XL line without ATc, whereas the growth of *ebl*-KD parasites was significantly reduced following ATc administration. Specifically, the parasitemia in the ATc(+) group was significantly lower than that in the ATc(-) group 12 h after ATc administration and was $< 10\%$ of that in the ATc(-) group 24 h after ATc administration (Fig. 4a). To determine which intraerythrocytic stage was affected, we classified the observed parasite morphologies into four developmental stages; namely, ring, small late trophozoite (diameter $< 50\%$ of host cell diameter), large late trophozoite (diameter $\geq 50\%$ of host cell diameter), and schizont (> 1 nucleus); and the proportion of each stage was calculated 0, 12, and 18 h after ATc administration. At all time points the proportion of the ring stage was the highest among the 4 stages in ATc(-) parasites. In contrast, the proportion of the ring stage dramatically decreased 12 h after ATc administration and that of the large late trophozoite and schizont stages increased in the ATc(+) group (Fig. 4b). We did not observe parasites with abnormal morphology on Giemsa-stained thin blood smears. These results suggest that the knockdown of *ebl* impedes the erythrocyte invasion step. The *in vitro* erythrocyte invasion assay using purified merozoites showed 1–2% parasitemia for the ATc(-) group, whereas it was significantly lower in the ATc(+) group (0.01–0.02%, Fig. 4c). These results clearly indicate that *ebl* is essential for erythrocyte invasion by *P. yoelii* merozoites within the timeframe of an ATc experiment.

3.5. *Ebl* is required to establish an irreversible connection with the erythrocyte by the *P. yoelii* 17XL line

To determine the erythrocyte invasion step affected by the knockdown of *ebl*, we performed time-lapse imaging analysis. Purified Tg1 and Tg2 line merozoites were mixed with mouse erythrocytes and recorded for approximately 40 min under a video microscope, then the numbers and duration of each invasion step were measured for erythrocyte interaction events. We categorized the sequential invasion steps as i) merozoite attachment, ii) erythrocyte deformation, and iii) echinocytosis (Fig. 5a selected from Videos 1 and 2). Only invasion events initiated within the first 25 min of the recording were selected (e.g., see video 1 for Tg1 without ATc, and Video 2 for Tg1 with ATc). For the *ebl*-KD Tg1 line, 25 and 76 merozoite attachments were observed without and with ATc, respectively. Among parasites that attached to the erythrocyte, 15 (60%) and 58 (76%) merozoites deformed erythrocytes without or with ATc, respectively. For the *ebl*-KD Tg2 line, 31 and 55 merozoite attachments were observed in ATc(-) and ATc(+) groups, respectively; and 29 (94%) and 47 (85%) merozoites deformed erythrocytes in ATc(-) and ATc(+) groups, respectively. There was no significant difference in the occurrence of deformation between the ATc(-) and ATc(+) groups (Fig. 5b). Significant difference was also not seen for the duration from the attachment to the beginning of the deformation between ATc(-) and ATc(+) groups for both *ebl*-KD lines (Fig. 5c). These results suggest that erythrocyte deformation mediated by merozoite interaction is independent of EBL expression. We observed 4 (27%) and 15 (52%) echinocytosis events among 15 and 29 merozoite deformations without ATc for the *ebl*-KD Tg1 and Tg2 lines, respectively, whereas no echinocytosis occurred for either line with ATc (Fig. 5b). This significant difference ($p < .01$ by two-tailed Fisher's exact test) further validates that EBL is required for successful erythrocyte invasion. We further noticed that merozoites with ATc appeared to frequently detach from the erythrocyte after its deformation. For the *ebl*-KD Tg1 line, detachment was observed for 4 out of 15 (27%) and 52 out of 58 (90%) merozoites that deformed erythrocytes in ATc(-) and ATc(+) groups, respectively. For *ebl*-KD Tg2 line, 7 out of 29 (24%) and 44 out of 47 (94%) merozoites detached in ATc(-) and

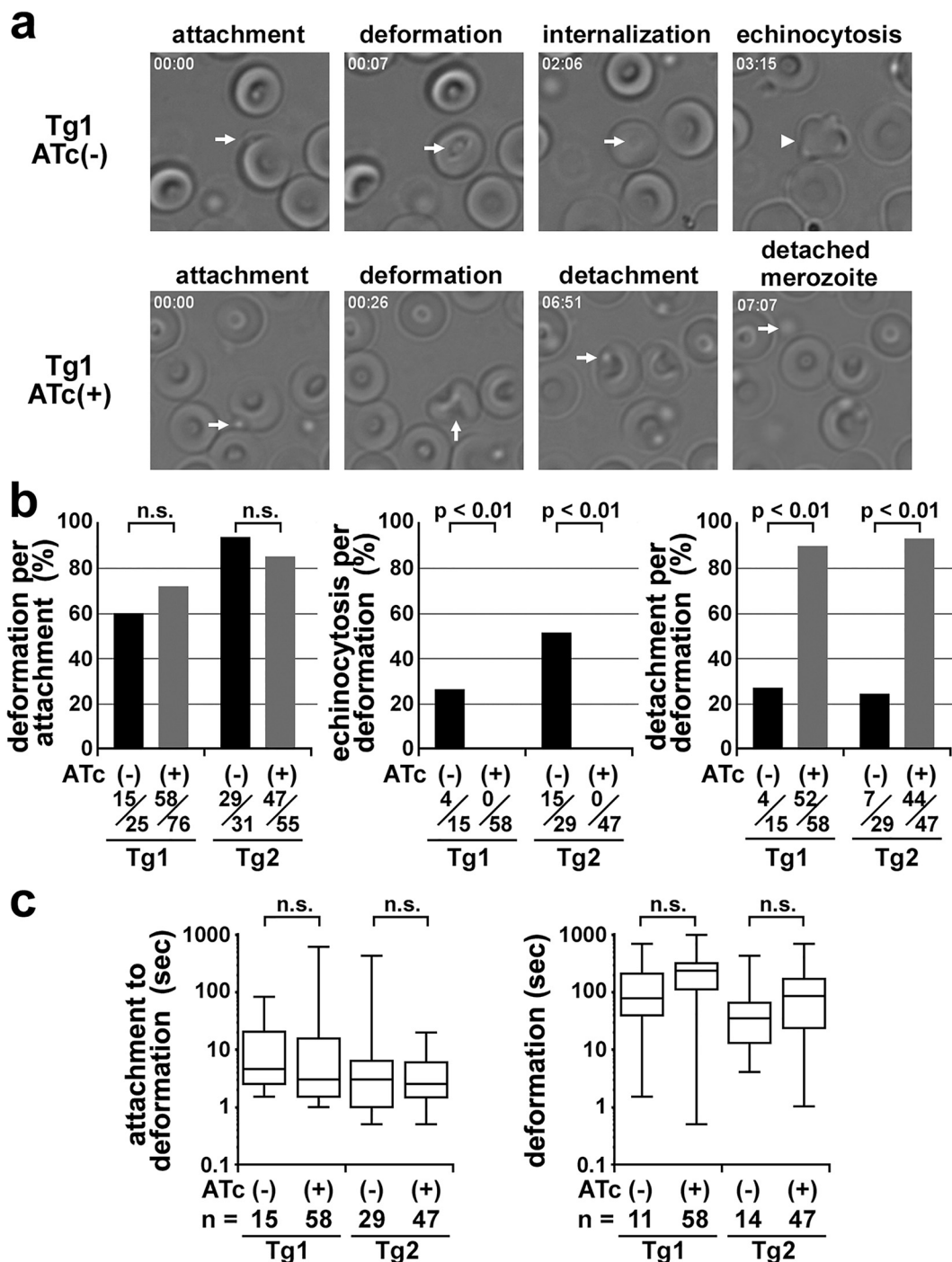
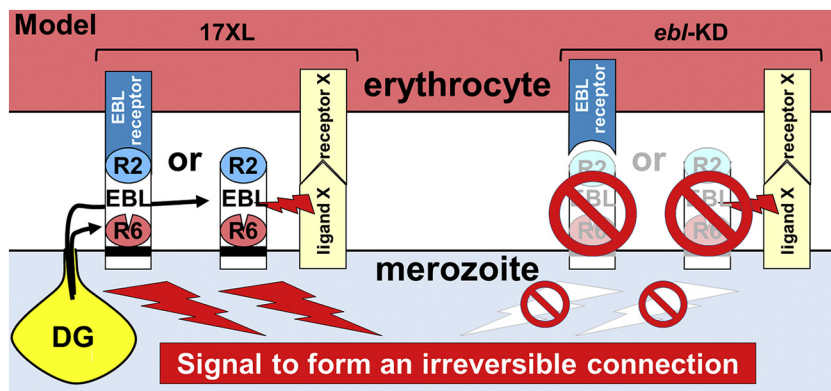


Fig. 5. Time-lapse imaging of erythrocyte invasion by *ebl*-KD parasites. (a) Representative images for erythrocyte invasion steps cropped from time-lapse videos. Merozoite attachment, erythrocyte deformation, internalization, echinocytosis and detached merozoite are shown for the ATc(–) and ATc(+) group of the Tg1 line. Arrow and arrowhead indicate the invading merozoite and the erythrocyte. (b) Percentage of the event per previous event (shown on the bottom for ATc(–) and ATc(+) groups of Tg1 and Tg2 lines) are plotted for deformation per merozoite attachment, echinocytosis per erythrocyte deformation, and merozoite detachment per erythrocyte deformation. Significances were evaluated by two-tailed Fisher’s exact test and are indicated above each graph; n.s. indicates not significant. (c) Median values and confidence intervals were plotted for the duration from attachment to the beginning of the erythrocyte deformation and for the deformation for ATc(–) and ATc(+) groups of the Tg1 and Tg2 lines. Events for which merozoites internalized were excluded to assess the duration of erythrocyte deformation. Both ends of the box indicate upper and lower quartiles, lines outside the box indicate the highest and lowest values, and dots indicate outliers. Significances were not detected by Mann-Whitney *U* test. n.s. indicates not significant.

ATc(+) groups, respectively. The occurrence of the detachment in the ATc(+) group was significantly greater ($p < .01$ by two-tailed Fisher’s exact test), suggesting that merozoites lacking EBL lose the ability to establish an irreversible connection with the erythrocyte (Fig. 5b). Significant difference was not detected for the duration of the

erythrocyte deformation between the ATc(–) and ATc(+) groups for both *ebl*-KD lines (Fig. 5c), suggesting that EBL is not involved in the erythrocyte deformation event before the internalization of merozoites.



ment. R2, region 2; R6, region 6.

4. Discussion

In this study we established for the first time the Tet-Off system in the *P. yoelii* rodent malaria parasite model system. Reduction of target *eb1* transcripts was $> 95\%$, consistent with transcript level reductions reported for the rodent malaria parasite *P. berghei* [19]. Our attempts to use the endogenous *eb1* promoter, as well as the *rhoph2* promoter, to establish an *eb1*-KD parasite line were unsuccessful. In contrast the *ron2* promoter allowed selection of a stable *eb1*-KD parasite line, suggesting that judicious selection of promoter strength driving TetR transcription is critical. Specifically, the *eb1* promoter is weaker than that for *ron2*, whereas the *rhoph2* is stronger than *ron2*. Genes other than *eb1* might be evaluated with the same strategy of testing a panel of constructs with promoters of different strengths for the appropriate life cycle stage of expression.

Time-lapse imaging analysis revealed that following *eb1*-knockdown in the 17XL line merozoites were unable establish an irreversible connection with the erythrocyte, consistent with electron microscopy descriptions that the proposed function of this family protein is to form a tight junction with the erythrocyte [8]. These results indicate that EBL in the 17XL line *P. yoelii*, and likely other *P. yoelii* lines, is required for tight junction formation, or an event immediately prior such as involvement in erythrocyte recognition. Because 17×1.1 pp. line parasites can survive despite the possible inability of their EBL to recognize erythrocytes, it is plausible that other erythrocyte recognizing molecule (s) participate in signal transduction. For example, upon interaction with the erythrocyte receptor, another merozoite surface ligand might transfer its signal to EBL, then the EBL cytoplasmic region, and thereby downstream molecules for rhoptry discharge required for tight junction formation. That said, it is formally possible that altered 17×1.1 pp. EBL gained an ability to recognize a wider range of erythrocytes. Recognition of erythrocyte surface glycoprotein A by EBA-175 was shown to trigger the secretion of rhoptry body proteins in *P. falciparum* [26]. This suggests that rhoptry neck (RON) proteins are also released from the merozoites, which are responsible to form an AMA1-RON complex located at the irreversible moving junction between the invading merozoite and erythrocyte membrane [27, 28]. It is of interest to determine whether RON proteins are secreted from the *eb1* knockdown parasites, once a method is established to evaluate rhoptry discharge in *P. yoelii*.

We show that the 17XL line translocates EBL to the merozoite surface, despite aberrant trafficking of EBL to dense granules in this line (Fig. 1). Because EBL signals are confined to one area on the merozoite surface in both 17XL and 17XNL lines, EBL may be located at the apical end in 17XL line as expected for 17XNL line. This suggests that the above hypothesized EBL-dependent signal transduction route is likely intact. Although it is possible that the merozoite surface EBL cannot recognize erythrocytes, we think this is unlikely because (1) the sequence of the EBL region 2 erythrocyte-binding domain is identical between the 17XL and 17XNL lines, and (2) recombinant region 2 of *P.*

Fig. 6. A model of the EBL function in *P. yoelii* 17XL line. EBL with altered region 6 (R6) in the 17XL line *P. yoelii* traffics to and is secreted from dense granules (DG), then either recognize its receptor on the erythrocyte (left) or receive signals from another merozoite surface ligand (ligand X) upon its erythrocyte receptor (receptor X) recognition (right) and transfer the signal to downstream molecules. The latter scenario of a role of EBL beside directly recognizing the erythrocyte is based on the evidences that 17×1.1 pp. line is able to survive even EBL region 2 erythrocyte binding domain appears to lose its ability [17], but still EBL is essential for the irreversible connection with the erythrocyte. EBL knockdown parasites (*eb1*-KD) without EBL are not able to establish an irreversible connection with erythrocytes, suggesting the lack of the EBL-independent signaling pathway for rhoptry discharge within the timeframe of an ATc knockdown experi-

vivax and *P. falciparum* EBL homologs are able to bind erythrocytes, when expressed on the surface of mammalian cells or as recombinant protein in *E. coli* [29–31]. Thus it is possible that the increased ability to invade a wider range of erythrocytes by the 17XL line is due to an increased amount of EBL translocated to the merozoite surface from “dense granules” that are larger than “micronemes”. For example, gene duplication of one of the Duffy Binding Protein (PkDBP α) in *Plasmodium knowlesi*, which would express double amount of PkDBP α , was reported to be linked to the increased invasion activity of *P. knowlesi* [32]. Alternatively it is also possible that other merozoite ligands compensate for EBL (Fig. 6), as described for 17×1.1 pp. line in the previous paragraph.

The reticulocyte-binding-like (RBL) proteins [33] are candidate merozoite surface ligands which might be capable of transferring signals to EBL family proteins. When *P. falciparum* Dd2 line parasites are maintained with sialic acid (SA)-negative erythrocytes, the SA-dependent ligand EBA-175 is unable to recognize erythrocytes, and the growth rate is transiently decreased. The recovery in growth is mediated by transcriptional upregulation of the RBL protein, RH4, which is an erythrocyte ligand independent of SA [34, 35]. This indicates that EBL and RBL family proteins are compensatory, whereas our data suggest that the two classes of receptors might not be interchangeable and, rather, a more complex mechanism is involved. It should be noted here, however, that although our ATc experiments demonstrated that *P. yoelii* merozoites lacking EBL are unable to invade erythrocytes, the ATc experimental design does not allow longer timeframes (specifically, revertant parasites emerged 72 h after ATc administration) and thereby study of possible epigenetic switching to an alternative invasion phenotype.

Our group has reported a time-lapse imaging method to analyze the dynamics of erythrocyte invasion by *P. yoelii* merozoites; however, in this procedure the prolonged and variable length of the interval of merozoite egress from the infected erythrocyte limits the number of invasion events that can be examined under the microscope [4]. We circumvented this limitation by using merozoites purified and stored at 15°C , which enabled $> 50\%$ of merozoites to survive for 4 h, before mixing with erythrocytes for microscopic assay [23]. Furthermore, incubation of schizonts *in vitro* at 15°C for 3 h was found to increase the number of fully matured schizonts available for merozoite purification. As a result, we were able to capture up to 76 erythrocyte invasion events in one time-lapse imaging procedure. Successful erythrocyte invasion, from attachment until echinocytosis, was observed in approximately 16 or 48% (Tg1 or Tg2, respectively) of the merozoites that attached to the erythrocyte without ATc. This method of merozoite purification coupled with time-lapse imaging allows quantitative and qualitative analysis of erythrocyte invasion events, and should be a useful tool to evaluate the mode of action of invasion inhibitory compounds and antibodies during erythrocyte invasion.

In conclusion, we established transgenic parasite lines in which *eb1*

expression can be conditionally knocked down by the Tet-Off system. We improved a time-lapse imaging procedure to capture erythrocyte invasion by *P. yoelii*, so that we are now able to simultaneously monitor numerous erythrocyte invasion events and quantitatively analyze invasion phenotype. Using this method, we convincingly showed that *eb1* is involved in the establishment of an irreversible connection between the merozoite and the erythrocyte.

Supplementary data to this article can be found online at <https://doi.org/10.1016/j.parint.2018.07.006>.

Following merozoite attachment, the erythrocyte was deformed, but echinocytosis did not occur and finally the merozoite detached from the erythrocyte. The *P. yoelii* *eb1*-KD Tg1 line was used for this video.

Acknowledgements

We are grateful to Soldati-Favre D and Pino P for plasmids. We also thank Templeton TJ for critical reading. This study was conducted at the Joint Usage / Research Center on Tropical Disease, Institute of Tropical Medicine, Nagasaki University, Japan. YK is a recipient of the Nagasaki University leading program scholarship and Rotary Club scholarship. TI is a recipient of the Japanese Society of Promotion Sciences (JSPS) DC1 scholarship. This work was supported in part by the Grants-in-Aids for Scientific Research 25293102 and 16H05184 (O.K.), for JSPS Fellows 17J09408 (T.I.), and for Scientific Research on Innovative Areas 23117008 (O.K.), MEXT, Japan. The funders have no role in study design, data collection and analysis, decision to publish, or preparation of the manuscript.

References

- World Health Organization, World Malaria Report, World Health Organization, 2017, Switzerland, Geneva, 2017.
- A.F. Cowman, B.S. Crabb, Invasion of red blood cells by malaria parasites, *Cell* 124 (2006) 755–766, <https://doi.org/10.1016/j.cell.2006.02.006>.
- G.E. Weiss, P.R. Gilson, T. Taechalerpaisarn, W.H. Tham, N.W.M. de Jong, K.L. Harvey, F.J.I. Fowkes, P.N. Barlow, J.C. Rayner, G.J. Wright, A.F. Cowman, B.S. Crabb, Revealing the sequence and resulting cellular morphology of receptor-ligand interactions during *Plasmodium falciparum* invasion of erythrocytes, *PLoS Pathog.* 11 (2015) 1–25, <https://doi.org/10.1371/journal.ppat.1004670>.
- K. Yahata, M. Treeck, R. Culleton, T.-W. Gilberger, O. Kaneko, Time-lapse imaging of red blood cell invasion by the rodent malaria parasite *Plasmodium yoelii*, *PLoS One* 7 (2012) e50780, <https://doi.org/10.1371/journal.pone.0050780>.
- A.F. Cowman, D. Berry, J. Baum, The cellular and molecular basis for malaria parasite invasion of the human red blood cell, *J. Cell Biol.* 198 (2012) 961–971, <https://doi.org/10.1083/jcb.201206112>.
- P.R. Gilson, B.S. Crabb, Morphology and kinetics of the three distinct phases of red blood cell invasion by *Plasmodium falciparum* merozoites, *Int. J. Parasitol.* 39 (2009) 91–96, <https://doi.org/10.1016/j.ijpara.2008.09.007>.
- X. Gao, K. Gunalan, S. Shu, L. Yap, P.R. Preiser, Triggers of key calcium signals during erythrocyte invasion by *Plasmodium falciparum*, *Nat. Commun.* 4 (2013) 1–11, <https://doi.org/10.1038/ncomms3862>.
- L.H. Miller, M. Aikawa, J.G. Johnson, T. Shiroishi, Interaction between cytochalasin B-treated malarial parasites and erythrocytes. Attachment and junction formation, *J. Exp. Med.* 149 (1979) 172–184, <https://doi.org/10.1084/jem.149.1.172>.
- A.P. Singh, H. Ozwara, C.H.M. Kocken, S.K. Puri, A.W. Thomas, C.E. Chitnis, Targeted deletion of *Plasmodium knowlesi* Duffy binding protein confirms its role in junction formation during invasion, *Mol. Microbiol.* 55 (2005) 1925–1934, <https://doi.org/10.1111/j.1365-2958.2005.04523.x>.
- J.H. Adams, B.K. Sim, S.A. Dolan, X. Fang, D.C. Kaslow, L.H. Miller, A family of erythrocyte binding proteins of malaria parasites, *Proc. Natl. Acad. Sci. U. S. A.* 89 (1992) 7085–7089, <https://doi.org/10.1073/pnas.89.15.7085>.
- D. Camus, T. Hadley, A *Plasmodium falciparum* antigen that binds to host erythrocytes and merozoites, *Science* 230 (1985) 553–556, <https://doi.org/10.1126/CVI.00082-10>.
- A.G. Maier, M.T. Duraisingh, J.C. Reeder, S.S. Patel, J.W. Kazura, P.A. Zimmerman, A.F. Cowman, *Plasmodium falciparum* erythrocyte invasion through glycophorin C and selection for Gerbich negativity in human populations, *Nat. Med.* 9 (2002) 87–92, <https://doi.org/10.1038/nm807>.
- D.C.G. Mayer, L. Jiang, R.N. Achur, I. Kakizaki, D.C. Gowda, L.H. Miller, The glycophorin C N-linked glycan is a critical component of the ligand for the *Plasmodium falciparum* erythrocyte receptor BAEBL, *Proc. Natl. Acad. Sci. U. S. A.* 103 (2006) 2358–2362, <https://doi.org/10.1073/pnas.0510648103>.
- D.C.G. Mayer, J. Cofie, L. Jiang, D.L. Hartl, E. Tracy, J. Kabat, L.H. Mendoza, L.H. Miller, Glycophorin B is the erythrocyte receptor of *Plasmodium falciparum* erythrocyte-binding ligand, EBL-1, *Proc. Natl. Acad. Sci. U. S. A.* 106 (2009) 5348–5352, <https://doi.org/10.1073/pnas.0900878106>.
- I. Landau, P. Gautret, in: L.W. Sherman (Ed.), *Malaria: Parasite biology, pathogenesis, and protection*, American Society for Microbiology, Washington, DC, 1998, pp. 401–417.
- H. Otsuki, O. Kaneko, A. Thongkukiatkul, M. Tachibana, H. Iriko, S. Takeo, T. Tsuboi, M. Torii, Single amino acid substitution in *Plasmodium yoelii* erythrocyte ligand determines its localization and controls parasite virulence, *Proc. Natl. Acad. Sci. U. S. A.* 106 (2009) 7167–7172, <https://doi.org/10.1073/pnas.0811313106>.
- H.M. Abkhallo, A. Martinelli, M. Inoue, A. Ramaprasad, P. Xangsayarath, J. Gitaka, J. Tang, K. Yahata, A. Zougrana, H. Mitaka, A. Acharjee, P.P. Datta, P. Hunt, R. Carter, O. Kaneko, V. Mustonen, C.J.R. Illingworth, A. Pain, R. Culleton, Rapid identification of genes controlling virulence and immunity in malaria parasites, *PLoS Pathog.* 13 (2017) 1–24, <https://doi.org/10.1371/journal.ppat.1006447>.
- R. Culleton, O. Kaneko, Erythrocyte binding ligands in malaria parasites: Intracellular trafficking and parasite virulence, *Acta Trop.* 114 (2010) 131–137, <https://doi.org/10.1016/j.actatropica.2009.10.025>.
- P. Pino, S. Sebastian, E.A. Kim, E. Bush, M. Brochet, K. Volkman, E. Kozlowski, M. Llinás, O. Billker, D. Soldati-Favre, A tetracycline-repressible transactivator system to study essential genes in malaria parasites, *Cell Host Microbe* 12 (2012) 824–834, <https://doi.org/10.1016/j.chom.2012.10.016>.
- C. Fernandez-Becerra, M.F. de Azevedo, M.M. Yamamoto, H.A. del Portillo, *Plasmodium falciparum*: New vector with bi-directional promoter activity to stably express transgenes, *Exp. Parasitol.* 103 (2003) 88–91, [https://doi.org/10.1016/S0014-4894\(03\)00065-1](https://doi.org/10.1016/S0014-4894(03)00065-1).
- G.G. Van Dooren, M. Marti, C.J. Tonkin, L.M. Stimmler, A.F. Cowman, G.I. McFadden, Development of the endoplasmic reticulum, mitochondrion and apicoplast during the asexual life cycle of *Plasmodium falciparum*, *Mol. Microbiol.* 57 (2005) 405–419, <https://doi.org/10.1111/j.1365-2958.2005.04699.x>.
- T. Sakura, K. Yahata, O. Kaneko, The upstream sequence segment of the C-terminal cysteine-rich domain is required for microneme trafficking of *Plasmodium falciparum* erythrocyte binding antigen 175, *Parasitol. Int.* 62 (2013) 157–164, <https://doi.org/10.1016/j.parint.2012.12.002>.
- J.K. Mutungi, K. Yahata, M. Sakaguchi, O. Kaneko, Isolation of invasive *Plasmodium yoelii* merozoites with a long half-life to evaluate invasion dynamics and potential invasion inhibitors, *Mol. Biochem. Parasitol.* 204 (2015) 26–33, <https://doi.org/10.1016/j.molbiopara.2015.12.003>.
- C.J. Janse, J. Ramesar, A.P. Waters, High-efficiency transfection and drug selection of genetically transformed blood stages of the rodent malaria parasite *Plasmodium berghei*, *Nat. Protoc.* 1 (2006) 346–356, <https://doi.org/10.1038/nprot.2006.53>.
- J.K. Mutungi, K. Yahata, M. Sakaguchi, O. Kaneko, Expression and localization of rhoptry neck protein 5 in merozoites and sporozoites of *Plasmodium yoelii*, *Parasitol. Int.* 63 (2014) 794–801, <https://doi.org/10.1016/j.parint.2014.07.013>.
- S. Singh, M.M. Alam, I. Pal-Bhowmick, J.A. Brzostowski, C.E. Chitnis, Distinct external signals trigger sequential release of apical organelles during erythrocyte invasion by malaria parasites, *PLoS Pathog.* 6 (2010), <https://doi.org/10.1371/journal.ppat.1000746>.
- J. Cao, O. Kaneko, A. Thongkukiatkul, M. Tachibana, H. Otsuki, Q. Gao, T. Tsuboi, M. Torii, Rhoptry neck protein RON2 forms a complex with microneme protein AMA1 in *Plasmodium falciparum* merozoites, *Parasitol. Int.* 58 (2009) 29–35, <https://doi.org/10.1016/j.parint.2008.09.005>.
- M.L. Tonkin, M. Roques, M.H. Lamarque, M. Pugnieri, D. Dougnet, J. Crawford, M. Lebrun, M.J. Boulanger, Host cell invasion by apicomplexan parasites: insights from the co-structure of AMA1 with a RON2 peptide, *Science* 333 (2011) 463–467, <https://doi.org/10.1126/science.1204988>.
- C.E. Chitnis, L.H. Miller, Identification of the erythrocyte binding domains of *Plasmodium vivax* and *Plasmodium knowlesi* proteins involved in erythrocyte invasion, *J. Exp. Med.* 180 (1994) 497–506, <https://doi.org/10.1084/jem.180.2.497>.
- B.K. Sim, C.E. Chitnis, K. Wasniowska, T.J. Hadley, L.H. Miller, Receptor and ligand domains for invasion of erythrocytes by *Plasmodium falciparum*, *Science* 264 (1994) 1941–1944, <https://doi.org/10.1126/science.8009226.3>.
- T.M. Tran, A. Moreno, S.S. Yazdani, C.E. Chitnis, J.W. Barnwell, M.R. Galinski, Detection of a *Plasmodium vivax* erythrocyte binding protein by flow cytometry, *Cytometry Part A* 63A (2005) 59–66, <https://doi.org/10.1002/cyto.a.20098>.
- S. Dankwa, C. Lim, A.K. Bei, R.H. Jiang, J.R. Abshire, S.D. Patel, J.M. Goldberg, Y. Moreno, M. Kono, J.C. Niles, M.T. Duraisingh, Ancient human sialic acid variant restricts an emerging zoonotic malaria parasite, *Nat. Commun.* 7 (2016) 11187, <https://doi.org/10.1038/ncomms11187>.
- W.H. Tham, J. Healer, A.F. Cowman, Erythrocyte and reticulocyte binding-like proteins of *Plasmodium falciparum*, *Trends Parasitol.* 28 (2012) 23–30, <https://doi.org/10.1016/j.pt.2011.10.002>.
- O. Kaneko, J. Mu, T. Tsuboi, X. Su, M. Torii, Gene structure and expression of a *Plasmodium falciparum* 220-kDa protein homologous to the *Plasmodium vivax* reticulocyte binding proteins, *Mol. Biochem. Parasitol.* 121 (2002) 275–278, [https://doi.org/10.1016/S0166-6851\(02\)00042-7](https://doi.org/10.1016/S0166-6851(02)00042-7).
- J. Stubbs, K.M. Simpson, T. Triglia, D. Plouffe, C.J. Tonkin, M.T. Duraisingh, A.G. Maier, E.A. Winzler, A.F. Cowman, Molecular mechanism for switching of *P. falciparum* invasion pathways into human erythrocytes, *Science* 309 (2005) 1384–1387, <https://doi.org/10.1126/science.1115257>.